# Hydroelasticity of slender bodies in an unbounded fluid in the medium frequency range

F. Chabas, Christian Soize

# HYDROELASTICITY OF SLENDER BODIES IN AN UNBOUNDED FLUID IN THE MEDIUM FREQUENCY RANGE

by

F. CHABAS (*) and C. SOIZE (**)

## ABSTRACT

We study in this paper the feasibility, in the medium frequency domain, of a slender body asymptotic formulation, for the hydro-elasto-acoustic calculations, previously developed in the low frequency range.

For a slender body with an axisymmetrical outer surface, submersed in an unbounded compressible fluid, this formulation deals with the construction of the hydrodynamic coupling and radiation operators.

We give a criteria that determines the frequency domain of validity of the theory as a function of the circumferential and longitudinal wave numbers $n$ and $m$ and for a given geometry of the structure. The analysis of this domain for physical structures shows that the theory may be extended as is to the MF range for the subspaces $n>0$ but has to be replaced by the general formulation for the subspace $n=0$, in this frequency range.

Special programs have been developed to take this distinction into account, the tests validating these programs show the efficiency of the method from a numerical point of view.

Keywords (NASA thesaurus): Structural analysis − Hydroelasticity − Slender bodies.

(*) ONERA Research Engineer.
(**) ONERA Head of Research Group.

# I. – INTRODUCTION

In order to situate the problem examined herein, we briefly summarize below the analysis methods developed for hydroelastoacoustic calculation in the low frequency (LF) and medium frequency (MF) domains at ONERA's Structures Department.

Let us consider a linear, viscoelastic, solid medium with instantaneous memory (the structure) which occupies an open bounded domain $\Omega_e$ of $\mathbb{R}^3$ with a relatively regular boundary $\partial\Omega_e = \Sigma \cup \Gamma$. The surface $\Sigma$ is in contact with an inviscid compressible fluid which occupies the open, unbounded domain $\Omega$ of $\mathbb{R}^3$. We note as $N$ the unit vector normal to $\partial\Omega_e$ external to $\Omega_e$ (Fig. 1).
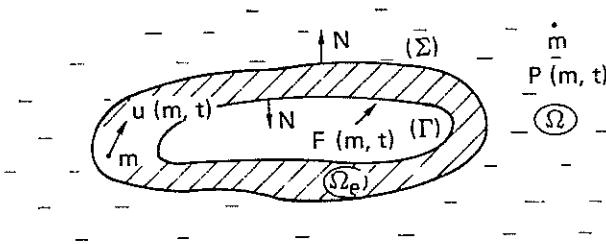


Fig. 1. – Diagram of the coupled fluid-structure system.

Let $u(m, t)$ be the displacement field of the elastic medium $\Omega_e$ and $F(m, t)$ be a surface force field applied on $\partial\Omega_e$. We will note as $p(m, t)$ the pressure field in the fluid $\bar{\Omega}$.

The equation for the linear vibrations of the coupled fluid-structure system are around a position of static equilibrium written in the Fourier domain for the time variable $t$ :

$$\forall \omega \in \mathbb{R}, \quad (-\omega^2 M + i\omega C + K - \omega^2 B_H(\omega))\, \hat{u}(\omega) = \hat{F}(\omega) \quad (1)$$

where $M$, $C$ and $K$ are the positive-definite symmetrical, real linear operators of mass, damping and stiffness of the elastic medium $\Omega_e$ and $B_H(\omega)$ is the linear hydrodynamic coupling operator which expresses the actions of the fluid on the structure when surface $\Sigma$ is deformed. This operator $B_H(\omega)$ which depends only on the fluid density $\rho_F$, the speed of sound $c_F$ in the fluid and the geometry of surface $\Sigma$ in the reference configuration, is symmetrical, complex (but not Hermitian) and can be written:

$$\forall \omega \in \mathbb{R}, \quad -\omega^2 B_H(\omega) = -\omega^2 M_H(\omega) + i\omega C_H(\omega) \quad (2)$$

where $M_H(\omega)$ and $C_H(\omega)$ are the added mass and dissipation by radiation at infinity operators and are positive-definite, symmetrical, real, linear operators.

The pressure $\hat{p}(m, \omega)$ in any point $m$ of $\bar{\Omega}$ is then given by the equation:

$$\hat{p}(m, \omega) = -\omega^2 Q_m(\omega)\, \hat{u}|_{\Sigma}(\omega) \quad (3)$$

where $\hat{u}|_{\Sigma}$ is the restriction on $\Sigma$ of the solution $\hat{u}$ of (1) and $Q_m(\omega)$ is the hydrodynamic radiation operator which also depends only on $\rho_F$, $C_F$ and $\Sigma$.

All the operators introduced have infinite dimension and, for any geometry of $\Omega_e$ (and therefore of $\Sigma$), only approximations can be constructed using appropriate methods.

## A. – SOLVING OF THE COUPLING EQUATION

The general method for approximating operators $M$, $C$, $K$ and $B_H(\omega)$ consists of projecting them on a suitable functional basis $\{ b_k(m) \}_{k \in \mathbb{N}}$ derived from the weak formulation of the coupling equation (1). We then attempt to find the solution $\hat{u}$ of (1) with the form:

$$\hat{u}(m, \omega) = \sum_{k=1}^{+\infty} \hat{U}_k(\omega)\, b_k(m), \\ m \in \bar{\Omega}_e, \quad \omega \in \mathbb{R} \quad (4)$$

The approximation consists of conserving only $n$ vectors of basis $b_k$, where $n$ is finite and the approximated solution is obtained by solving the matrix equation on $\mathbb{C}^n$:

$$(-\omega^2 [\tilde{M}] + i\omega [\tilde{C}] + [\tilde{K}] - \omega^2 [\tilde{B}_H(\omega)]) [\hat{U}] = [\hat{F}]$$

where:

$$[\tilde{M}]_{kk'} = \ll M b_{k'}, b_k \gg \\ [\tilde{C}]_{kk'} = \ll C b_{k'}, b_k \gg \\ [\tilde{K}]_{kk'} = \ll K b_{k'}, b_k \gg \\ [\hat{U}]_k = \hat{U}_k \\ [\hat{F}]_k = ((\hat{F}, b_{k | \partial\Omega_e}))_{\partial\Omega_e} \\ [\tilde{B}_H(\omega)]_{kk'} = ((B_H(\omega) b_{k' | \Sigma}, b_{k | \Sigma}))_{\Sigma} \quad (6)$$

$$\ll v, w \gg = \int_{\Omega_e} \langle v(m), w(m) \rangle\, dm \\ ((v, w))_S = \int_S \langle v(m), w(m) \rangle\, dS(m) \quad (7)$$

where $\langle v, w \rangle$ is the Euclidian scalar product of $v$ and $w$ on $\mathbb{R}^3$.

The various methods developed are related both to the selection of basis $b_k$ and to the method used to compute $[\tilde{B}_H(\omega)]_{kk'} = ((B_H(\omega) b_{k' | \Sigma}, b_{k | \Sigma}))_{\Sigma}$.

The criteria involved in this choice are:

— the LF or MF frequency domain for the choice of basis $b_k$;

— the geometric characteristics of $\Sigma$ for the calculation of $[\tilde{B}_H(\omega)]$.

## A.1. — Selection of bases $b_k$

(a) In the LF domain, two methods have been developed:

— The first consists of taking for $b_k$ the eigenmodes of vibration $\psi_k$ of the elastic medium, conservative in a vacuum. They are such that:

$$-\omega_k^2\, M\,\psi_k + K\,\psi_k = 0. \qquad (8)$$

These eigenmodes are numerically determined by the finite element method.

For the LF domain, a very small number of modes is sufficient, i.e. $n$ is less than a hundred. This method is developed and used in [4, 5, 9, 14, 23 (1) and (2)].

The second consists of taking for $b_k$ the eigenmodes of vibration $\psi_k^F$ of the conservative elastic medium placed in the associated bounded incompressible fluid medium. They are such that:

$$-\omega_k^2\, (M + M_H(0))\,\psi_k^F + K\,\psi_k^F = 0. \qquad (9)$$

Here again, the modes are numerically determined by the finite element method (structure and fluid) and truncation can be carried out for the LF domain with a small value of $n$. The advantage of the second method is that the $\psi_k^F$ values already account for the major part of the influence of the added mass. This method normally leads to a smaller value of $n$ than the first. However, the calculation of (9) is more cumbersome than that of (8) since the model also includes the degrees of freedom of the fluid. This method is described in [19 and 21].

(b) In the MF domain, calculation of bases $\psi_k$ and $\psi_k^F$ becomes very difficult or even impossible in the present state of numerical analysis and the most powerful computers (this is due to the fact that the modal densities become large and there may be several hundred or several thousand modes to be calculated).

This is why we developed a direct approach which uses the finite element basis used for modeling the structure. In this case, it is not necessary first to solve an eigenvalue problem of type (8) or (9), but $n$ is very large since it is actually the number of degrees of freedom of the structure model and the mesh is relatively fine for the MF domain ($n$ is equal to several tens of thousands). This method is described in [23 (3), 24, 25, 26 (1) to (3)].

## A.2. — Selection of the method for computing $[\tilde{B}_H(\omega)]$

Operator $B_H(\omega)$ results from solving the external Neumann problem in unbounded domain $\Omega$, related to Helmholtz's equation relative to bounded surface $\Sigma$. A method which is well suited to this type of problem consists of using the formulation by integral equations. We will limit ourselves herein to this approach, which applies both to the LF domain and the MF domain.

(a) For a surface $\Sigma$ of $\mathbb{R}^3$ with any geometry, which is the general case, a singularities method, which gets around the problem of irregular frequencies, was developed. It is described in [1] and is used in [5 (1) and (2), 9, 14 (1) and (2), 25, 26 (1) to (3)] both for the LF and the MF domain. It can process any bounded surface $\Sigma$ of $\mathbb{R}^3$ and a free surface in $\Omega$ can be taken into account.

(b) For a slender surface $\Sigma$, use of this geometric property can be considered to develop a method for constructing $B_H(\omega)$ at a lower cost than with the general method mentioned above in point (a).

Such an approach was developed for slender axisymmetrical surfaces $\Sigma$ in the LF domain (for the coupled problem, this does not require the elastic body $\Omega_e$ to be of revolution; only $\Sigma$ must be). The results obtained are developed in detail in [23 (1)], summarized in [4] and the comparisons with general numerical methods and experimental measurements are very good [20, 23 (2)]. These results were established mathematically and were only validated for the LF domain. In [24], we studied to what extent the LF results could be extended to the MF domain and how they should be modified.

We give these results below.

## B. RADIATION CALCULATION

After solving the coupling equation (5), the radiation is obtained considering (3) by the following approximation:

$$\hat{p}(m,\ \omega) = -\omega^2 \sum_{k=1}^{n} \hat{U}_k(\omega)\, (Q_m(\omega)\, b_{k\,|\,\Sigma}). \qquad (10)$$

The construction of operator $Q_m(\omega)$ projected on traces $b_{k\,|\,\Sigma}$ of the basis vectors is carried out at the same time as the construction of $[\tilde{B}_H(\omega)]$ by the methods mentioned above in point A.2.

## C. — ORIENTATION OF THIS PAPER

As was already explained, the purpose is to replace the general 3D method for constructing hydrodynamic operators $B_H(\omega)$ and $Q_m(\omega)$ by a simplified method, less costly from a numerical standpoint, when surface $\Sigma$ is slender and axisymmetrical.

In [24], we demonstrated that it was possible to extend the mathematical results obtained for the LF domain in [23 (1) and (2)] to any frequency domain

and accordingly to the MF domain. Thus, regardless of the reduced wave number $K = \dfrac{\omega L}{C_F}$ *fixed*, where $L$ is the length of $\Sigma$, the asymptotic result obtained in [23 (1) and (2)] remains valid when the slenderness parameter $\varepsilon = \dfrac{R_{max}}{L}$ approaches 0, where $R_{max}$ is the largest radius of the surface of revolution $\Sigma$.

Unfortunately, the asymptotic result is not uniform in $K$, *i.e.* for $K$ fixed, there exists $\varepsilon_0(K)$ such that $\forall \varepsilon < \varepsilon_0(K)$, the asymptotic result applies. However, in real situations, the opposite problem is posed. The slender structure, and therefore surface $\Sigma$, is given and has a fixed slenderness parameter $\varepsilon$ (which is in the neighborhood of 1/5 to 1/15), which means that it is not possible to make it approach zero. Therefore, if the coupled problem is studied for a wide range of values of $K$, it is necessary to know the domain for which the asymptotic theory is valid. This analysis of the domain of validity was conducted and led us to modify the asymptotic theory for the MF domain.

We give the main results obtained below, referring the reader to [24] for demonstrations.

## II. — HYPOTHESES AND NOTATIONS

The notations and hypotheses introduced in paragraph I are taken.

The system is referenced in a fixed cartesian reference frame $OXYZ$ of $\mathbb{R}^3$. A generic point of $\mathbb{R}^3$ is represented by its cylindrical coordinates $(X, R, \theta)$ in the cylindrical reference system with axis $OX$ associated with $OXYZ$. The distance between two points $m(X, R, \theta)$ and $m'(X', R', \theta')$ is noted $\rho(m, m')$ or again:

$$\rho(X-X', R, R', \theta-\theta') = [(X-X')^2$$
$$+ R^2 + R'^2 - 2RR'\cos(\theta-\theta')]^{1/2}. \quad (11)$$

The following hypotheses are introduced:

H1 — The linearized problem around a reference configuration is analyzed.

The 3D displacement field of surface $\Sigma$ is noted $U_\Sigma(m, t)$, $m \in \Sigma$.

This field is not particular and is not necessarily axisymmetrical.

H2 — Surface $\Sigma$ is axisymmetrical, with an axis of revolution $OX$ and a finite length $L$. Its generatrix is described by the function $X \mapsto R_0(X)$ defined on $[0, L]$ with values in $\mathbb{R}^+$, assumed sufficiently regular for $\Sigma$ to be $C^1$. Thus, for any point $m$ of $\Sigma$, the unit vector $N$ normal to $\Sigma$ inside $\Omega$ can be defined, if function $m \mapsto N(m)$ is continuous. We set:

$$\dot{R}_0(X) = dR_0(X)/dX, \qquad h(X) = (1 + \dot{R}_0(X)^2)^{1/2}. \quad (12)$$

Actually, hypothesis $C^1$ can be weakened by taking $\Sigma$ as type $C^0$ and $C^1$ by parts. The numerical analysis developed in [24] is based on this weakened hypothesis. The programs developed thereby allow sharp angles to be taken into account.

The slenderness hypothesis of surface $\Sigma$ is written:

$$\varepsilon = R_{max}/L \ll 1, \qquad R_{max} = \sup_{X \in [0, L]} R_0(X). \quad (13)$$

H3 — The fluid is inviscid and compressible with constant density $\rho_F$. The speed of propagation, assumed constant, of sound in the fluid is noted $C_F$ and the velocity field is noted $V(m, t)$, $m \in \Omega$. Under these conditions, for any point $m \in \Omega$, a velocity potential $\Phi(m, t)$ can be defined such that:

$$V(m, t) = \mathrm{grad}_m \Phi(m, t) \quad (14)$$

and the pressure is written:

$$P(m, t) = -\rho_F \frac{\partial \Phi}{\partial t}(m, t). \quad (15)$$

## III. — EXTERNAL NEUMANN PROBLEM RELATED TO HELMHOLTZ'S EQUATION (case of any surface)

It is attempted to find the harmonic solution with the form:

$$u_\Sigma(m, t) = \hat{u}_\Sigma(m, \omega) e^{i\omega t} \quad (16)$$

$$\Phi(m, t) = \hat{\varphi}(m, \omega) e^{i\omega t} \quad (17)$$

$$p(m, t) = \hat{p}(m, \omega) e^{i\omega t} \quad (18)$$

where $m \mapsto \hat{u}_\Sigma(m, \omega)$ [or $m \mapsto \hat{\psi}(m, \omega)$, $m \mapsto \hat{p}m, \omega)$] is defined on $\Sigma$ (or on $\bar{\Omega}$) with values in $\mathbb{C}^3$ (or in $\mathbb{C}$). Considering equation (15), this gives:

$$\hat{p}(m, \omega) = -i\omega\rho_F \hat{\varphi}(m, \omega). \quad (19)$$

Under these conditions, $\hat{\varphi}$ is the solution of the following external Neumann problem:

$$\Delta\hat{\varphi} + \frac{\omega^2}{C_F^2}\hat{\varphi} = 0 \quad \text{dans } \Omega \quad (20)$$

$$\frac{\partial\hat{\varphi}}{\partial N}(m, \omega) = F(m, \omega) \quad \text{sur } \Sigma \quad (21)$$

$$\left. \begin{aligned} \left| \frac{\partial\hat{\varphi}}{\partial N}(m, \omega) - i\frac{\omega}{C_F}\hat{\varphi}(m, \omega) \right| &= \theta\left(\frac{1}{r^2}\right), \\ \left| \hat{\varphi}(m, \omega) \right| &= \theta\left(\frac{1}{r}\right) \end{aligned} \right\} \quad (22)$$

for

$$r = \| 0m \| \rightarrow +\infty$$

setting:

$$F(m, \omega) = i\omega \langle \hat{u}_\Sigma(m, \omega), N(m) \rangle \quad (23)$$

where $m \mapsto F(m, \omega)$ is a function defined on $\Sigma$ with values in $\mathbb{C}$.

For any $\omega$ fixed in $\mathbb{R}$ and any function $m \mapsto F(m, \omega)$ in $C^0(\Sigma, \mathbb{C})$, problem (20) to (22) accepts a unique solution $\hat{\varphi}$ continuous in $\bar{\Omega}$ (and even in $\mathbb{R}^3$) which is written:

$$\hat{\varphi}(m, \omega) = (\mathscr{R}_\omega(F))(m), \qquad m \in \bar{\Omega}$$

where $\mathscr{R}_\omega$ is a linear operator of $C^0(\Sigma, \mathbb{C})$ in $C^0(\bar{\Omega}, \mathbb{C})$.

The hydrodynamic coupling operator $B_H(\omega)$ is then defined by:

$$((B_H(\omega)\hat{u}_\Sigma, \bar{\hat{v}}_\Sigma))_\Sigma$$

$$= -\rho_F \int_\Sigma \langle \bar{\hat{v}}_\Sigma, N \rangle \{ \mathscr{R}_\omega(\langle \hat{u}_\Sigma, N \rangle) \} \, d\sigma \quad (25)$$

where $d\sigma$ is the measure of the surface borne by $\Sigma$. The radiation operator $Q_m$ is defined by:

$$Q_m(\omega)\hat{u}_\Sigma = -\rho_F \mathscr{R}_\omega(\langle \hat{u}_\Sigma, N \rangle)(m). \quad (26)$$

Let $G(m, m')$ be the elementary solution of Helmholtz's equation in $\mathbb{R}^3$ which verifies:

$$\Delta G_\omega(m, m') + \frac{\omega^2}{C_F^2} G_\omega(m, m') = \delta_m, \ (m) \quad (27)$$

and compatible with (22). It is written:

$$G_\omega(\rho(m, m')) = -\frac{1}{4\pi} \frac{e^{-i(\omega/C_F)\rho(m, m')}}{\rho(m, m')} \quad (28)$$

setting $G_\omega(m, m') = G_\omega(\rho(m, m'))$.

Then, the solution of (20) to (22) can be searched for in the form of a single layer $v_\omega \otimes \delta_\Sigma$, where $m \mapsto v_\omega(m)$ is continuous on $\Sigma$; this then gives:

$$\forall m \in \bar{\Omega}, \qquad \hat{\varphi}(m, \omega)$$

$$= \int_\Sigma v_\omega(m') G_\omega(m, m') \, d\sigma(m'). \quad (29)$$

The density of single layer $v_\omega$ borne by $\Sigma$ is then a solution of the integral equation associated with (29):

$$\forall m \in \Sigma, \qquad F(m, \omega) = \frac{1}{2} v_\omega(m)$$

$$+ \int_\Sigma v_\omega(m') \frac{\partial G_\omega(m, m')}{\partial N(m)} \, d\sigma(m'). \quad (30)$$

It is known that equation (30) does not have a solution for certain values $\omega \in \mathbb{R}$ called irregular frequencies, whereas problem (20) to (22) always has a solution $\forall \omega \in \mathbb{R}$. In the present case, this is not a problem since form (30) is used only to find the asymptotic solution ($\varepsilon \to 0$) which is explicitly obtained for any $\omega \in \mathbb{R}$.

## IV. — THE RESULTS FOR A SLENDER SURFACE $\Sigma$ OF REVOLUTION

We now consider the hypothesis of paragraph II, introducing the dimensionless wave number:

$$K = \omega L / C_F. \quad (31)$$

For any $m \in \Sigma$, the linear operator $\mathscr{U}_{\varepsilon, m}$ is defined such that for any $m \mapsto v(m)$ continuous on $\Sigma$:

$$\mathscr{U}_{\varepsilon, m}(v) = \int_\Sigma v(m') \frac{\partial G_\omega(m, m')}{\partial N(m)} \, d\sigma(m'). \quad (32)$$

The asymptotic solution is then given by (29) with $v_\omega$ a solution of (30) for $\varepsilon \to 0$, i.e.:

$$\forall m \in \Sigma, \qquad F(m, \omega) = \frac{1}{2} v_\omega(m) + \lim_{\varepsilon \to 0} \mathscr{U}_{\varepsilon, m}(v_\omega). \quad (33)$$

Result 1. — *For any 3D Neumann condition with the form* $F(X, \theta, \omega) = F_n(X, \omega) e^{in\theta}$, $n \in \mathbb{Z}$, *then the single layer density is written* $v_\omega(X, \theta) = v_{\omega, n}(X) e^{in\theta}$ *and,* $\forall D > 0$ *fixed,* $\forall K > 0$ *fixed, there exists* $\varepsilon_0(K)$ *such that* $\forall \varepsilon \leq \varepsilon_0(K)$, *for any $X$ in $[0, L]$:*

$$\left| \mathscr{U}_{\varepsilon, X}(v_{\omega, n}) - \frac{1}{2} \frac{1_0(n)}{h(X)} v_{\omega, n}(X) \right| \leq D \quad (34)$$

*where* $1_0(n) = 1$ *if* $n = 0$ *and* $1_0(n) = 0$ *if* $n \neq 0$.

Result 2. — *For any 3D Neumann condition* $X, \theta \mapsto F(X, \theta, \omega)$ *continuous on* $[0, L] \times [0, 2\pi]$, *then* $\forall D > 0$ *fixed and* $\forall K > 0$ *fixed, there exists* $\varepsilon_0(K)$ *such that* $\forall \varepsilon \leq \varepsilon_0(K)$, *for any* $m \in \bar{\Omega}$:

$$\left| \mathscr{R}_\omega(F)(m) - \tilde{\mathscr{R}}_\omega(F)(m) \right| \leq D \quad (35)$$

*where*

$$(\tilde{\mathscr{R}}_\omega(F))(X, R, \theta)$$

$$= \int_0^L \int_0^{2\pi} \mathscr{A}_{X', \theta'}(F) G_\omega(\rho(X - X', R,$$

$$R_0(X'), \theta - \theta')) \, d\sigma(X', \theta') \quad (36)$$

$$d\sigma(X', \theta') = R_0(X') h(X') dX' \, d\theta' \quad (37)$$

*and where* $\mathscr{A}_{X', \theta'}$ *is the linear operator defined, for any fixed $X'$ and $\theta'$, by:*

$$\mathscr{A}_{X', \theta'}(F) = 2 F(X', \theta', \omega)$$

$$- \left( \frac{1}{2\pi} \int_0^{2\pi} F(X', \theta'', \omega) d\theta'' \right) \left( \frac{2}{1 + h(X')} \right). \quad (38)$$

The proofs of these two results are given in [24] and [23 (1)].

*Comments on the results*

For any function $S_n$ in $C^0([0, L], \mathbb{C})$, the operator $\mathcal{U}_{\epsilon, x}$ is written:

$$\mathcal{U}_{\epsilon, X}(S_n) = \int_0^L S_n(X') g_{\epsilon, n}(X, X') dX' \qquad (39)$$

The expression of $g_{\epsilon, n}$ is given in [24]. Result 1 shows that for any $K$ positive fixed and for any $X$ in $[0, L]$, $\mathcal{U}_{\epsilon, X}(S_n)$ approaches, not uniformly with respect to $K$, 0 if $n > 1$ and $S(X)/2h(X)$ if $n = 0$, when $\epsilon \to 0$.

This is due to the fact that for $\epsilon \to 0$, $g_{\epsilon, n}(X, X')$ approaches 0 for $n > 1$ and the measure $\delta_X(X')/2h(X)$ for $n = 0$, where $\delta_X(X')$ is the Dirac measure at point $X$.

For $\epsilon$ fixed and small, an equivalent of $g_{\epsilon, n}(X, X')$ is calculated in [23 (1)]. The numerical analysis of this equivalent allows the following interpretation to be given:

(a) *Case $n = 0$*

For $\epsilon$ fixed and small and $X$ fixed, the function $X' \mapsto g_{\epsilon, 0}(X, X')$ has a graph like that shown in Figure 2.
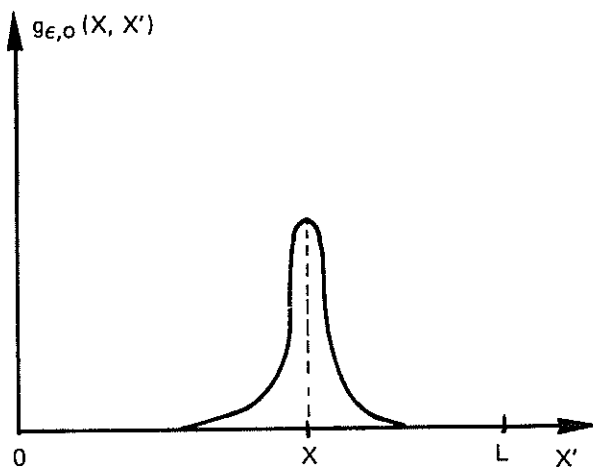


Fig. 2. — Graph of the function $g_{\epsilon, 0}(X, 0)$.

The smaller $\epsilon$, the more the mass of measure $g_{\epsilon, 0}(X, X') dX'$ is concentrated in point $X$. At the limit, for $\epsilon \to 0$, this gives, as we indicated, the Dirac measure on point $X$ within a constant. Thus, for $\epsilon$ fixed and small, in order to be able to use the asymptotic results, the function $X' \mapsto S_0(X')$ must be constant on the window defined by $g_{\epsilon, 0}$, *i.e.* it must be possible to write:

$$\int_0^L S_0(X') g_{\epsilon, 0}(X, X') dX' \simeq$$

$$S_0(X) \int_0^L g_{\epsilon, 0}(X, X') dX'. \qquad (40)$$

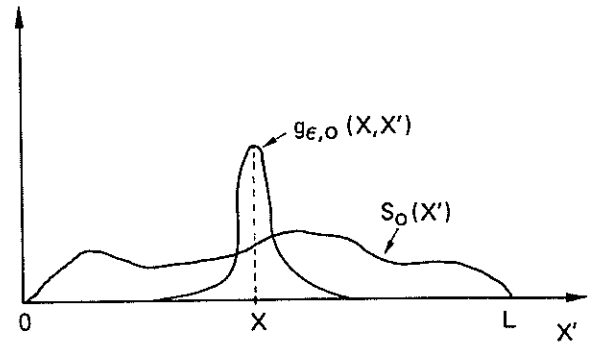This situation is illustrated in Figure 3.



Fig. 3. — Correct asymptotic situation.

However, when $K$ increases, which is the MF or HF situation, with $\epsilon$ still fixed and small, function $S_0$ generally oscillates increasingly and equation (40) is no longer verified. This situation occurs when the spatial wavelength associated with $S_0$ is of the same order of magnitude or less than the efficient width of the window (Fig. 4).
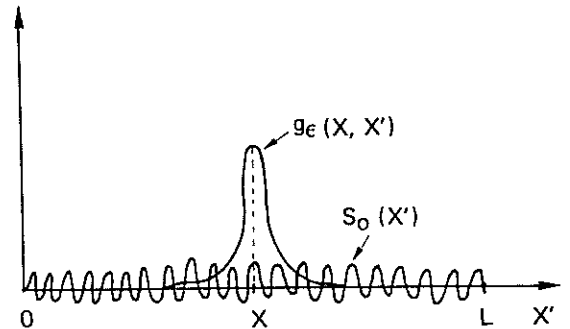


Fig. 4. — Incorrect asymptotic situation.

At the limit, if the spatial wavelength approaches zero, reasoning on the stationary phase shows that $\mathcal{U}_{\epsilon, X}(S_0)$ approaches zero, as in the case where $n > 1$.

Consequently, the character of the convergence towards the asymptotic solution, not uniform in $K$, implies the following practical conclusions for $n = 0$: for $\epsilon$ fixed, there is a change in the behavior of the solution as a function of $K$ and there is a wide range of values of $K$ about which nothing can be said. It is almost hopeless to wish to select the type of solution. In effect, for any Neumann condition, the wave spectrum of the contribution $n = 0$ which is written:

$$\hat{S}_0(k) = \int_0^L e^{ikX} S_0(X) dX \qquad (41)$$

can simultaneously have significant values for small values of $k$ (situation of Figure 3), for large values of $k$ (situation of Figure 4) and for intermediate values of $k$. This situation is encountered, for instance, when the vibrations of surface $\Sigma$ are longitudinally localized in space. Therefore, for $n = 0$, the asymptotic result can no longer be used unless $\epsilon$ is very small,

in accordance with result 1. But, as we will see in the next paragraph when studying the domain of validity, this leads to values of ε which do not correspond to real structures. Thus, for $n=0$ we are therefore led to dropping the asymptotic result in the MF domain. We will come back to this point.

*(b) Case $n > 1$*

However, for $n \geqq 1$, $g_{\varepsilon,n}(X, X')$ approaches zero and the problem does not occur. On the contrary, as we will see, the higher $K$, the better the asymptotic result. Actually, for $n > 1$, the convergence is uniform in $K$.

## REMARKS

Another way of interpreting these results is to note, according to (34), that the single layer does not have a spatial memory in the direction of slenderness $X$ if surface $\Sigma$ is sufficiently slender. This result, similar to the strip theory, means that the circumferential integral of the sources in a section with abscissa $X$ is not modified by the adjacent section with abscissa $X + dX$.

Thus, (33) and (34) show that for $n > 1$, the integral of the sources of a section is compensated for to a certain extent, since the deformation of $\Sigma$ is then isovolumic. The equivalent source of the section is then equal to twice the Neumann condition, whereas for $n=0$, as the deformation of $\Sigma$ involves a variation in volume, there is no compensation in a section and the source equivalent to a section is equal to only once the Neumann condition (within the curvature).

It is this lack of compensation in a section for $n=0$ which means that the solution does not converge uniformly in $K$ and that for ε fixed, the longitudinal spatial memory reoccurs for certain values of $K$, although it does not occur when $\varepsilon \to 0$, for any fixed $K$.

## V. — ANALYSIS OF THE DOMAIN OF VALIDITY

We now propose to establish a domain of validity for the theory, i. e. to find a criterion giving pairs $(\varepsilon, K)$ [or $(\varepsilon_0(K), K)$] which verify the asymptotic result (34).

To do so, we first define parameterizing as follows.

Helmholtz's equation (20) is written as follows in dimensionless variables and cylindrical coordinates $(R = R_{max} r, X = L x)$:

$$\frac{\partial^2 \tilde{\varphi}}{\partial r^2} + \frac{1}{r}\frac{\partial \tilde{\varphi}}{\partial r} + \frac{1}{r^2}\frac{\partial^2 \tilde{\varphi}}{\partial \theta^2} + \varepsilon^2 \frac{\partial^2 \tilde{\varphi}}{\partial x^2} + \varepsilon^2 K^2 \tilde{\varphi} = 0. \quad (42)$$

Let us assume that $\tilde{\varphi}(x, r, \theta)$ has the form:

$$\left. \begin{array}{l} \tilde{\varphi}(x, r, \theta) = F(r) e^{im\pi x} e^{in\theta}, \\ n \in \mathbb{N}, \quad m \in \mathbb{N}^* \end{array} \right\} \quad (43)$$

where $n$ is the circumferential wave number and $m$ the longitudinal wave number.

Substituting (43) in (42) gives:

$$\frac{d^2 F}{dr^2} + \frac{1}{r}\frac{dF}{dr} + \left[\varepsilon^2(K^2 - m^2\pi^2) - \frac{n^2}{r^2}\right]F(r) = 0. \quad (44)$$

Since $\sup_{x \in [0, 1]} r(x) = 1$, we will use as parameter:

$$\Gamma = \varepsilon^2(K^2 - m^2\pi^2) - n^2. \quad (45)$$

## A. — METHOD FOR EVALUATING THE DOMAIN

To simplify the calculations, we assume that $\Sigma$ has a constant radius.

Under these conditions, the operator $\mathcal{U}_{\varepsilon, x}$ defined by (32) has the following dimensionless expression:

$$\mathcal{U}_{\varepsilon, x}(s) = -\frac{\varepsilon^2}{2\pi}\int_0^1\int_0^\pi s(x')\cos(n\tau)$$
$$(1-\cos\tau)\left(-\frac{iK}{\rho_\varepsilon^2} - \frac{1}{\rho_\varepsilon^3}\right)e^{-ik\rho_\varepsilon}dx'\,d\tau \quad (46)$$

where

$$\rho_\varepsilon = [(x-x')^2 + 2\varepsilon^2(1-\cos\tau)]^{1/2} \quad (47)$$

and integral equation (30) becomes:

$$f(x) = \frac{1}{2}s(x) + \mathcal{U}_{\varepsilon, x}(s), \qquad x \in [0, 1]. \quad (48)$$

Evaluation of the domain consists of numerically calculating, for different values of parameters ε, $K$, $n$ and $m$, the "exact" value of $f$ by (46)-(48) for a given function $s$ and estimating the error between the exact solution and the asymptotic solution using the two following scalars:

$$C_0 = \frac{\|f - s\|}{\|f\|} \quad (49)$$

$$C_{\geqq 1} = \frac{\|f - (1/2)s\|}{\|f\|} \quad (50)$$

where $\| . \|$ represents the norm of $L^2([0, 1], \mathbb{R})$.

For the numerical calculation of (46), the integration domain $[0, 1] \times [0, \pi]$ is divided into rectangular blocks and quadrature is carried out by a method of $2D$ trapezoids. For each of the blocks containing the singularity, the integral is converted to polar coordinates and the integration is carried out on the polar

angle by a trapezoid method, the integration along the polar radius being carried out algebraically. All due precautions were taken as regards convergence of the quadrature as a function of the meshes.

The calculations were carried out for two types of source densities:

— $s(x) = \sin(m \pi x)$ which represents an unlocalized longitudinal deformation shape and allows estimation of the error in each point $k = m \pi$ of the wave spectrum of any function $s$;

— $s(x) = \dfrac{\sin m \pi (x - x_0)}{\pi (x - x_0)}$ which represents a deformation shape localized on the point with abscissa $x_0$ and is used to estimate the overall error for a function which has a rectangular window type wave spectrum where the width of the window is proportional to $m$.

## B. — THE RESULTS

The results are given in Figures 5 to 8 with a box showing the ranges of variation of the parameters used in calculation. Parameter $\Gamma$ is on the X-axis and the error constants $C_0$ and/or $C_{\geq 1}$ expressed as a percentage are on the Y-axis.
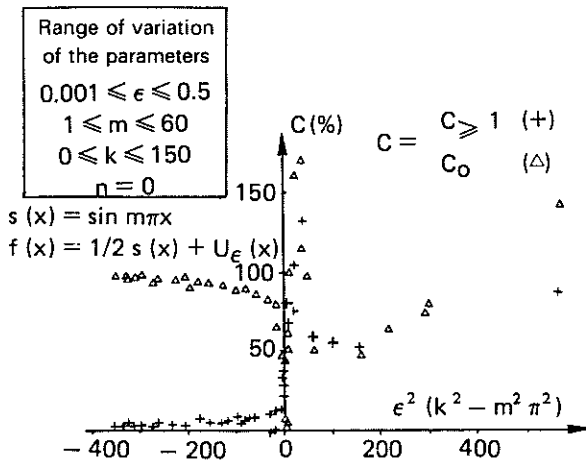


Fig. 5. — Validity domain for $n = 0$.
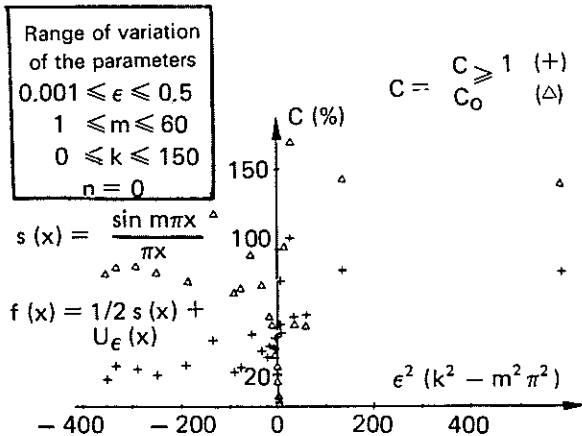Unlocalized deformation shape.



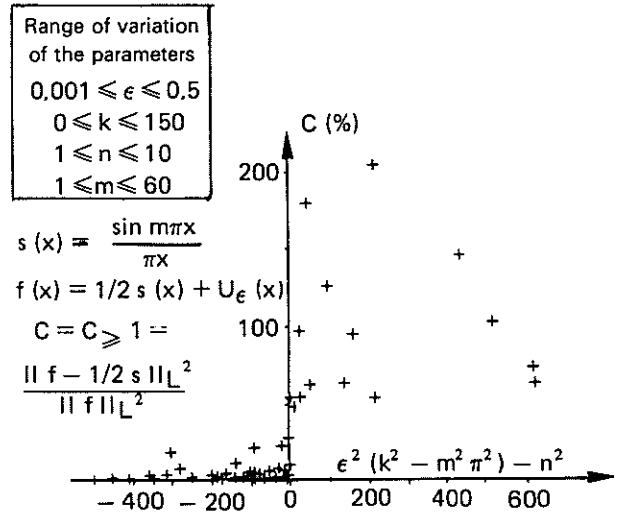Fig. 6. — Validity domain for $n = 0$.
Localized deformation shape.



Fig. 7. — Validity domain $n \geq 1$.
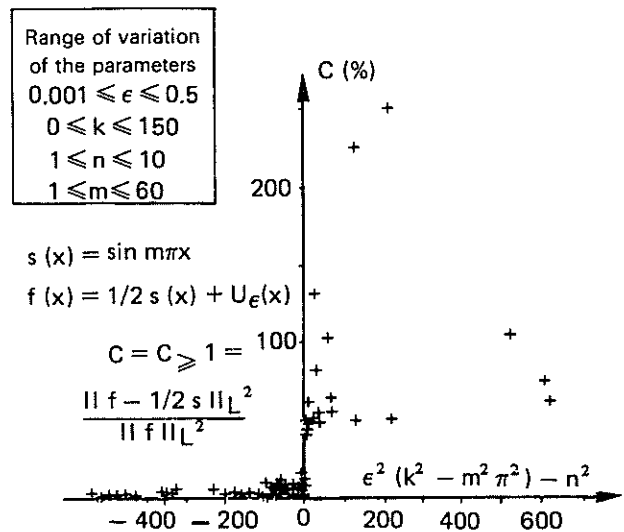Unlocalized deformation shape.



Fig. 8. — Validity domain for $n \geq 1$.
Localized deformation shape.

— For deformations of $\Sigma$ of the bending type $(n > 1)$, the validity criterion is written:

$$\varepsilon^2 (K^2 - m^2 \pi^2) - n^2 < 0 \qquad (51)$$

with, on the whole, an error below 5%.

This criterion shows, which is interesting, that for $K$ fixed, the larger $m$ and $n$, the higher $\varepsilon$ can be.

— For deformations of $\Sigma$ of the torsion and breathing type $(n = 0)$, the difficulties mentioned in Section IV arise, $i.e.$ a change in behavior of the solution.

To preserve the asymptotic result, the criterion is written:

$$\varepsilon^2 |K^2 - m^2 \pi^2| \ll 1. \qquad (52)$$

Unfortunately, for high values of $K$, this criterion generally leads to $\varepsilon$ too small to be applicable to real structures.

Therefore, although the asymptotic result is mathematically valid for $n=0$, it is of no practical use which leads us to construct the exact solution by the direct method for this case.

# VI. — METHOD FOR CONSTRUCTING OPERATORS

The hydrodynamic coupling operator is defined by (25).

## A. — CASE OF A FULLY AXISYMMETRICAL COUPLED SYSTEM

In this case, the displacement field $\hat{u}|_\Sigma(m, \omega)$ can be conventionally broken down, for its component normal to $\Sigma$, into a direct sum of subspaces, with the calculations made subspace by subspace.

For a field which is symmetrical with respect to $\theta=0$, this gives:

$$\langle \hat{u}|_\Sigma, N \rangle (X, R_0, \theta) = \sum_{n \geq 0} \hat{u}_n(X, R_0, \theta)$$
$$= \sum_{n \geq 0} \hat{u}_n^s(X, R_0) \cos n\theta. \quad (53)$$

Section V leads us to distinguish between two cases:
— For $n=0$, we have:

$$((B_H(\omega)\hat{u}|_\Sigma, \hat{v}_{|\Sigma}))_\Sigma = ((B_H^0(\omega)\hat{u}_0, \hat{v}_0))_\Sigma$$
$$= [\tilde{B}_H^0(\omega)\hat{u}_0^s, \hat{v}_0^s] \quad (54)$$

where $\tilde{B}_H^0$ is calculated by the general method developed in [1] and used in [5 (1) and (2), 9, 14 (1) and (2), 25, 26 (1) to (3)].
— For $n > 1$, we have:

$$((B_H(\omega)\hat{u}|_\Sigma, \hat{v}_{|\Sigma}))_\Sigma = ((B_H^n(\omega)\hat{u}_n, \hat{v}_n))$$
$$= [\tilde{B}_H^n(\omega)\hat{u}_n^s, \hat{v}_n^s] \quad (55)$$

where $\tilde{B}_H^n$ is calculated using the asymptotic result.

## B. — CASE OF THE COUPLED 3D SYSTEM

The Fourier series development (53) of the 3D field remains valid in this case. The coupling operator is constructed with the form:

$$B_H(\omega) = B_H^{\geq 1}(\omega) + \tilde{\tilde{B}}_H^0(\omega). \quad (56)$$

— $B_H^{\geq 1}(\omega)$ is the operator applied to the 3D field $\hat{u}|_\Sigma$ globally constructed by the asymptotic formula-

tion associated with the partial breakdown:

$$\langle \hat{u}|_\Sigma^{\geq 1}, N \rangle (X, R_0, \theta) = \sum_{n \geq 1} \hat{u}_n(X, R_0, \theta). \quad (57)$$

This operator is constructed from equation (36), algebraically removing the contribution of subspace $n=0$ in (38). It therefore does not involve calculation of the axisymmetrical operator $n=0$ by the asymptotic formulation.

$\tilde{\tilde{B}}_H^0(\omega)$ is the operator associated with subspace $n=0$ applied to the 3D field $\hat{u}|_\Sigma$. Insofar as it is not possible to "unfold" an asymmetrical operator, we propose the following approximation.

Let $\pi_0$ be the projection operator on subspace $n=0$ defined as follows for any function $(x, \theta) \mapsto F(X, \theta)$ continuous on $[0, 2\pi]$:

$$(\pi_0 F)(X) = \frac{1}{2\pi} \int_0^{2\pi} F(X, \theta') d\theta'. \quad (58)$$

Let $\tilde{B}_H^0$ be the operator defined by (54) calculated by the general method. By applying (58) to $\hat{u}_0^s$ and $\hat{v}_0^s$, $\tilde{B}_H^0$ defines an operator $\bar{B}_H^0$ applied to the 3D field which is informally expressed:

$$[\tilde{B}_H^0 \hat{u}_0^s, \hat{v}_0^s] = [\tilde{B}_H^0 \pi_0 \hat{u}|_\Sigma, \pi_0 \hat{v}|_\Sigma] = ((\bar{B}_H^0 \hat{u}|_\Sigma, \hat{v}_{|\Sigma}))_\Sigma. \quad (59)$$

The following approximation is proposed for $\tilde{\tilde{B}}_H^0$:

$$\tilde{\tilde{B}}_H^0(\omega) = \text{diag } \bar{B}_H^0(\omega) \quad (60)$$

i. e., we restrict operator $\bar{B}_H^0(\omega)$ to its diagonal. This approximation was justified empirically by observing that it gave fully satisfactory results.
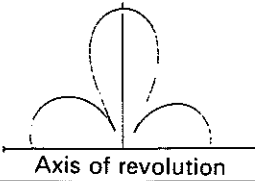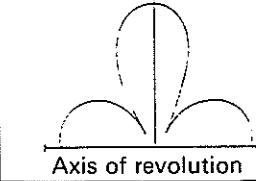
# VII. — EXAMPLES

General programs were developed from the formulation described in this paper to process axisymmetrical and 3D coupled systems. These programs calculate the discretized coupling and radiation operators on a finite element basis of the surface of the structure in contact with the fluid. Two calculation examples, one axisymmetrical and the other 3D, are given below to illustrate the theory and validate the programs developed.

## A. — AXISYMMETRICAL CALCULATION

The elastic structure is a cylindrical hull with a variable radius, closed at the ends, with an axis of revolution $Oz$. It is submerged in water and its slenderness is $\varepsilon=0.043$.

TABLE I

Calculation $n=0$

| Modal calculation (number of modes of the truncated base: 6) | Calculation by the finite element method with the coupling and radiation operators constructed by the general MF method |
|---|---|
| $F_{dry}=9.50$ | — |
| $F_{wet}=9.20$ | $F_{wet}=9.176$ |
| $\gamma_{max}=0.318.10^{-4}$ | $\gamma_{max}=0.318.10^{-4}$ |
| $P_{max}=0.1590$ | $P_{max}=0.1601$ |
| $\dfrac{P_{max}}{\gamma_{max}}=4990$ | $\dfrac{P_{max}}{\gamma_{max}}=4737$ |
|  |  |
| Axis of revolution | Axis of revolution |

The reference calculation is carried out by writing the coupling equations on the truncated modal base and locating the peak frequencies of the coupled system by a scattering method (*see* introduction). The first six modes in each subspace were used. The calculations illustrating the slender body theory use the results of Section VI. — A) and the MF methods
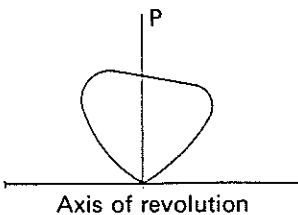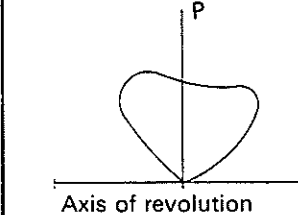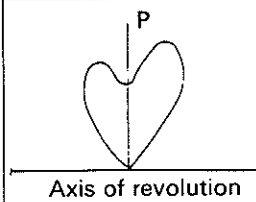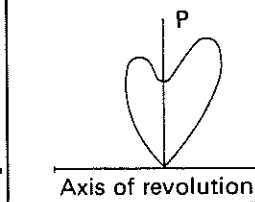
TABLE II

Calculation $n=1$

| Modal calculation (number of modes of the truncated base: 6) | Calculation by the finite element method with slender body model |
|---|---|
| $F_{dry}=13.60$ | — |
| $F_{wet}=11.08$ | $F_{wet}=10.845$ |
| $\gamma_{max}=0.409.10^{-4}$ | $\gamma_{max}=0.4005.10^{-4}$ |
| $P_{max}=0.55.10^{-1}$ | $P_{max}=0.404.10^{-1}$ |
| $\dfrac{P_{max}}{\gamma_{max}}=1343$ | $\dfrac{P_{max}}{\gamma_{max}}=1010$ |
|  |  |
| Axis of revolution | Axis of revolution |

TABLE III

Calculation $n=2$

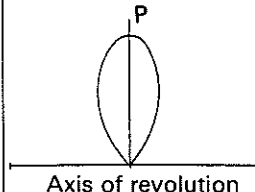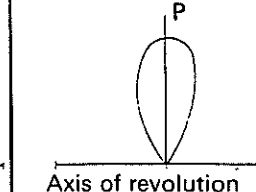| Modal calculation (number of modes of the truncated base: 6) | Calculation by the finite element method with slender body model |
|---|---|
| $F_{dry}=8.04$ | — |
| $F_{wet}=5.945$ | $F_{wet}=6.023$ |
| $\gamma_{max}=0.2841.10^{-4}$ | $\gamma_{max}=0.295.10^{-4}$ |
| $P_{max}=0.1841.10^{-2}$ | $P_{max}=0.1878.10^{-2}$ |
| $\dfrac{P_{max}}{\gamma_{max}}=65$ | $\dfrac{P_{max}}{\gamma_{max}}=64$ |
|  |  |
| Axis of revolution | Axis of revolution |

[26] for narrow bands with a width of 1 Hz centered on the peak frequency in water.

For each mode studied, the structural damping rate is $\xi=0.01$.

For both calculations, the finite elements of the structure are axisymmetrical 2D with eight nodes, with a nonaxisymmetrical displacement field. The fluid mesh includes 73 nodes on the generatrix and 18 nodes on the half-circumference in the modal calculation and 102 nodes on the half-circumference in the slender body calculation.

TABLE IV

Calculation $n=2$

| Modal calculation (number of modes of the truncated base: 6) | Calculation by the finite element method with slender body model |
|---|---|
| $F_{dry}=13.84$ | — |
| $F_{wet}=10.835$ | $F_{wet}=10.976$ |
| $\gamma_{max}=0.199.10^{-3}$ | $\gamma_{max}=0.2010.10^{-3}$ |
| $P_{max}=0.1583.10^{-1}$ | $P_{max}=0.1552.10^{-1}$ |
| $\dfrac{P_{max}}{\gamma_{max}}=79$ | $\dfrac{P_{max}}{\gamma_{max}}=77$ |
|  |  |
| Axis of revolution | Axis of revolution |

For each subspace, the unit local excitation with axis $Oy$ is applied so as to adapt to the mode analyzed.

The mechanical observations of the coupled system are the peak frequency in water, the normal wall acceleration and the far field pressure. The pressure calculation points are located on a circle in plane $Oyz$ centered on the structure and the results are converted to a distance $d = 1\,m$ from the center of the structure $\left(\text{for a decrease in pressure in } \dfrac{1}{d}\right)$.

All the results are given in tables I to IV and show excellent agreement between the two calculations. Concerning the calculation time, the gain achieved by the method proposed is greater than 10, in spite of a much finer circumferential modeling of the fluid.

## B. — 3D CALCULATION

The elastic structure is a cylindrical hull centered on point (0, 0, 0) with a constant radius, with axis of revolution $Oz$ closed at the ends by flat bottoms.

It is homogeneous, isotropic, with length $L = 120$, thickness $e = 0.02$, radius $R = 5$ and is submerged in water $(c = 1,500)$.

In this case, all the calculations are 3D. For construction of the coupling operator, the general method [1] is used for the reference calculation and the results of Section VI. — B) for the calculation by the slender body theory. The coupled system vibration equation is solved by the MF method for the 5-15 Hz analysis band. An analytic calculation of the eigenmodes of vibration in a vaccum of the associated conservative structure shows that the latter has more than 60 modes in this band, which is a typical MF situation.

For this analysis band, an average structural damping rate for the dry structure of $\xi = 0.003$ was used.

For both calculations, only a quarter of the structure was modeled, taking into account the two planes of symmetry with equations $x = 0$ and $z = 0$. Modeling of the dry structure, which includes 420 hull elements with 8 nodes, allows circumferential wave numbers up to nine to be taken into account. The discretization of the coupling operator includes 820 fluid panels using all the nodes of the structural mesh.

The symmetrical local excitation is applied to point $(0, R, 0)$ on axis $Oy$ and is equal to 0.25 for the modeled quarter of the structure.

Figure 9 shows the square of the acceleration modulus normal to the excitation point in decibels.
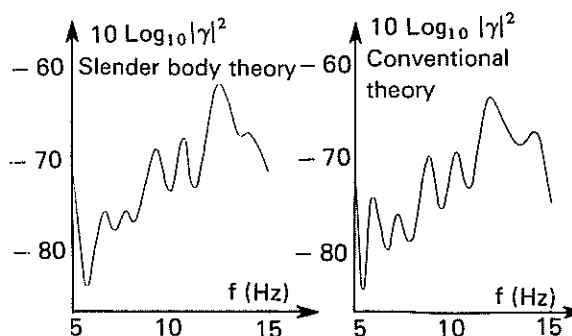


Fig. 9.

Comparison between the two calculations shows good agreement. They give the same levels, the only difference being a shift of approximately 1 Hz of the peak frequencies in water. However, the magnitude of this shift should be relativized. In effect, it should be stressed that the frequency domain analyzed was determined so as to obtain a model compatible with the structural deformation modes and the acoustic wavelengths in the fluid and leading to a reasonable number of degrees of freedom (in this case approximately 6000). This choice is actually very penalizing for comparison of the results, since the analysis band is very narrow considering the high modal density of the structure. In other words, very high frequency resolution is required.

Accordingly, the shift relative to the analysis band becomes minimal for a larger frequency domain (for instance 100 Hz).
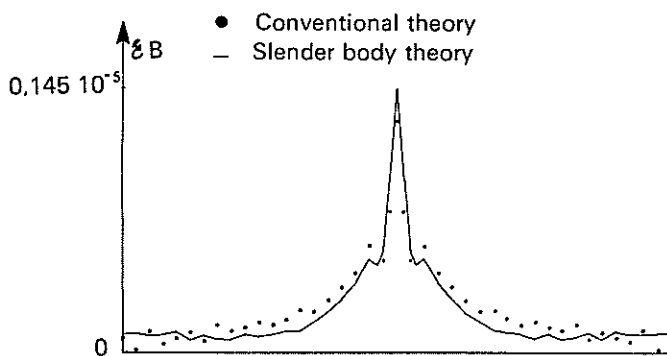


Fig. 10. – Longitudinal deformation shape.

Figures 10 and 11 show the deformation shapes of the structures in water on the generatrix and the directrix containing the excitation point. The quantity shown is the energy of the normal acceleration on the analysis band, defined by:

$$\mathscr{E}_B = \int_{\mathbb{R}} |\gamma(t)|^2\,dt = \frac{1}{2\pi}\int_B |\hat{\gamma}(\omega)|^2\,d\omega. \qquad (61)$$

The values are normalized with respect to the maximum energy on the structure.
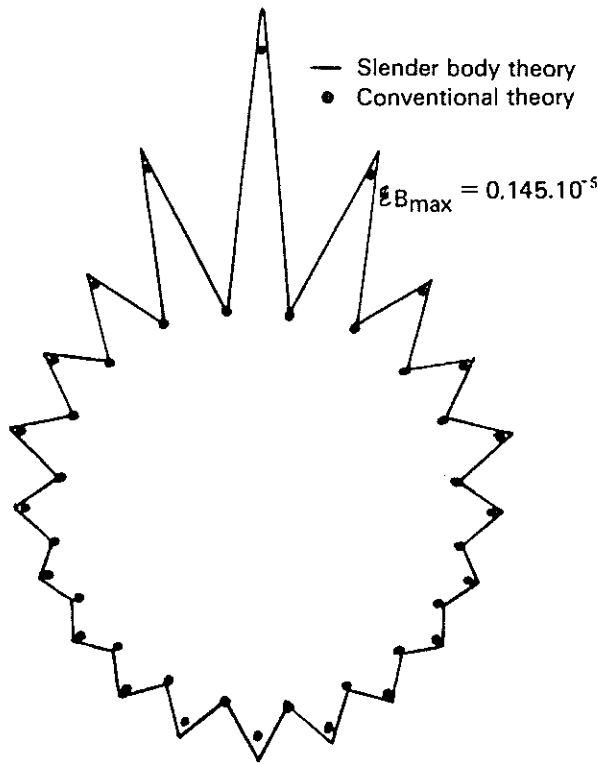
Fig. 11. − Circumferential deformation shape.

The spatial localization of the deformation shapes and the small longitudinal propagation of the energy show that it is an MF situation. Figure 10 shows the large couplings of the circumferential deformation modes.

Figures 12 to 14 show the far field pressure radiation patterns (the depth of immersion is 70 m from the free surface), in the planes with equation $x=0$, $y=0$ and $z=0$.
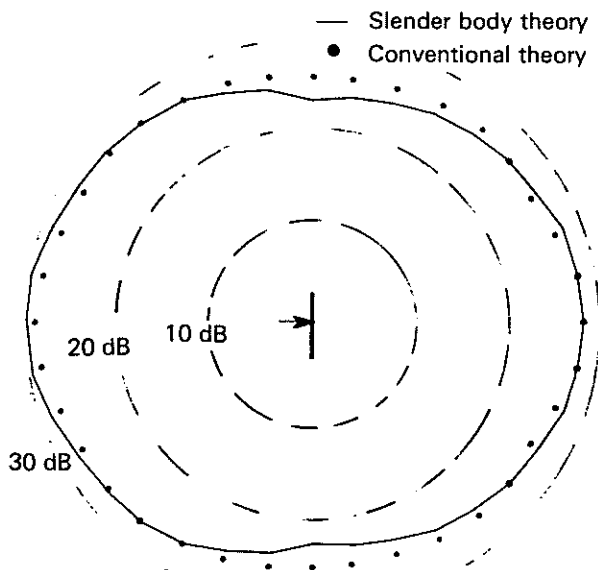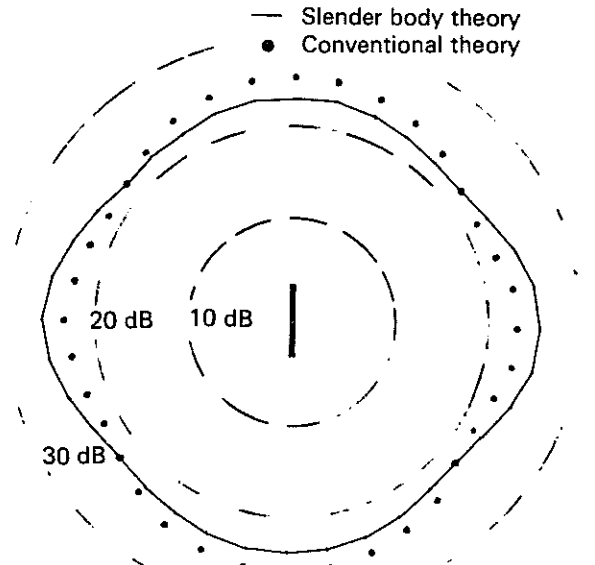


Fig. 12. − Far field pressure.  Plane $x=0$.



Fig. 13. − Far field pressure.  Plane $y=0$.
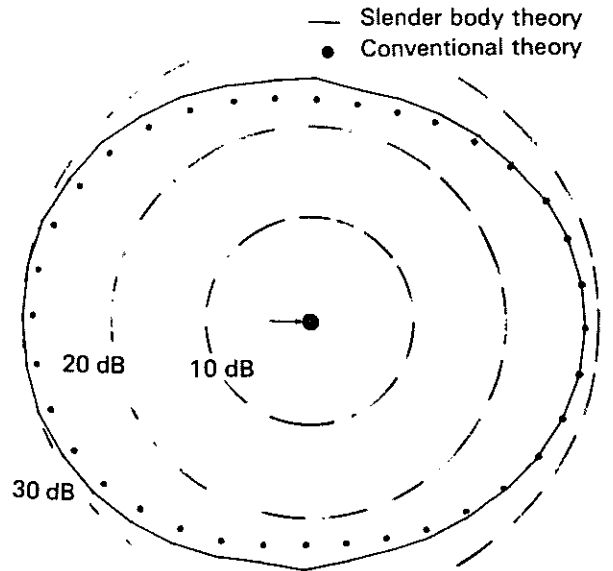


Fig. 14. − Far field pressure.  Plane $z=0$.

The quantity shown is the energy in decibels of the pressure on the analysis band expressed in micropascals, $i.\,e.$:

$$\mathscr{E}_P = 10\log_{10}\left\{\frac{1}{2\pi}\int_B |\hat{p}(\omega)|^2\,d\omega\right\} + 60. \quad (62)$$

The comparison between the two calculations shows a maximum relative difference of approximately 5% which is satisfactory considering approximation (60).

For this problem, the savings in calculation time for construction of the coupling operator by the slender body method is approximately 4. This gain increases with the size of the model and should be much higher for structures with a high number of degrees of freedom (20,000 or more).

# VIII. — CONCLUSION

In this paper, we showed how the slender body theory developed in [4] could be extended to the medium frequency domain, with the associated numerical developments used to solve the problems of hydroelastic coupling in an unbounded compressible fluid entering this framework.

The existence of a domain of validity of the theory was shown and a simple way was given for determining it for a given structure.

From the standpoint of applications to real structures, the theory can be extended as is to the MF domain for subspaces $n > 0$, but must be replaced by the general formulation for subspace $n = 0$ in this frequency range.

This result led us to develop special programs taking this distinction into account. The processing performed to validate the programs shows the efficiency of the method, which allows a significant decrease in calculation costs.

*Manuscript handed in on June 18, 1986*

# REFERENCES

[1] ANGELINI J. J. and HUTIN P. M. – *Problème extérieur de Neumann pour l'équation d'Helmoltz. La difficulté des fréquences irrégulières.* La Recherche Aérospatiale, n° 1983-3 French and English editions.

[2] BATHE K. J. and WILSON E. L. – *Numerical methods in finite element analysis.* Prentice Hall, (1976).

[3] BEALE J. J. – *Eigenfunction expansions for objects floating in open sea.* Communications on pure and applied mechanics, vol. 30, (1977).

[4] COUPRY G. and SOIZE C. – *Hydroelasticity and the field radiated by a slender body into an unbounded fluid.* Journal of Sound and Vibration (1984), 96 (3).

[5] DAVID J. M. – (1) *Calcul hydro-elasto-acoustique dans le domaine basse fréquence du SNLE M20 et de sa maquette au 1/10.* RT ONERA 33/3454 RY 083 R-084 R, (1984). (2) *Calcul hydro-élasto-acoustique tridimensionnel de la poutre tubulaire avec massif dans le domaine basse fréquence.* RT ONERA 36/3454 RY 080 R, (1984).

[6] DUVAUT G. and LIONS J. L. – *Les inéquations en mécanique et en physique.* Dunod, Paris, (1972).

[7] EUVRARD D. – *La théorie des corps élancés pour un navire avançant en eau calme.* Contrat DRET/ENSTA, Rapport de recherche ENSTA, n° 145, (1983).

[8] HILLE E. and PHILLIPS R. S. – *Functional analysis and semi-groups.* American Math. Society Coll. Publishing (31), (1948).

[9] HUTIN P. M. and ANGELINI J. J. – *Correlation du bruit rayonné par une coque immergée avec son état vibratoire.* RT ONERA 2/3454 RY 003 R, (1980).

[10] JOUAN A., MORVAN A. and ALLARDOT J. P. – *Essais hydro-élasto-acoustiques de la poutre tubulaire au lac de Castillon.* RT ONERA 18/3454 RY 040 R, (1982).

[11] JOUAN A., MORVAN A. and GUILLAUMIE L. – *Expérimentation élasto-acoustique de la poutre tubulaire en basse et moyenne fréquence au lac de Castillon.* RT ONERA 37/3454 RY 082-447 R, (1984).

[12] JUNGER M. C. and FEIT D. – *Sound structures and their interaction.* MIT Press, Cambridge.

[13] LANDAU L. D. and LIFCHITZ E. – *Fluid mechanics.* Pergamon Press, (1963).

[14] LAURENT A. – (1) *Étude du rayonnement du caisson Daphné 1/4 immergé dans le domaine basse fréquence.* RT ONERA 14/3454 RY 022 R, (1984). (2) *Identification hydro-élasto-acoustique de la poutre tubulaire en milieu semi-infini par la méthode des singularités.* RT ONERA 21/3454 RY 040 R, (1982).

[15] LAX P. D. and PHILLIPS R. S. – *Scattering theory.* Academic Press, New York, (1967).

[16] LIONS J. L. and MAGENES E. – *Problèmes aux limites non homogènes.* Dunod, Paris, (1968).

[17] MIKHLIN S. G. – *Mathematical physics and advanced course.* North Holland, (1970).

[18] MORSE P. M. and INGRID K. U. – *Theoretical acoustics.* McGraw Hill, N.Y., (1968).

[19] NICOLAS-VUILLERME B., OHAYON R. and VALID R. – *Vibrations harmoniques de structures élastiques immergées dans un liquide.* Publication de l'association technique, nautique et aéronautique, Paris, (1981).

[20] PIAZZOLI G. – *Rayonnement acoustique des coques.* RS ONERA 29/3454 RY 060 à 062 R, (1983).

[21] PIAZZOLI G. and OHAYON R. – *Rayonnement acoustique des structures sous-marines élastiques.* RS ONERA 26/3454 RY 050 à 052 R, (1983).

[22] ROSS D. – *Mechanics of underwater noise.* Pergamon Press, (1976).

[23] SOIZE C. – (1) *Hydro-élasticité des corps élancés de révolution dans un fluide compressible occupant un domaine non borné.* RT ONERA 17/3454 RY 052 R, (1982). (2) *Étude hydro-élasto-acoustique de la poutre tubulaire avec une théorie de corps élancé.* RT ONERA 20/3454 RY 002 R, (1982). (3) *Vibrations linéaires moyennes fréquences des structures élastiques anisotropes.* La Recherche Aérospatiale, n° 1982-5, French and English editions.

[24] SOIZE C. and CHABAS F. – *Hydrodynamique des corps élancés de révolution en fluide compressible non borné, dans le domaine MF.* RT ONERA 42/3454 RY 441 R, (1985).

[25] SOIZE C., HUTIN P. M., DESANTI A., DAVID J. M. and CHABAS F. – *Linear dynamic analysis of mechanical systems in the medium frequency range.* Journal of Computers and Structures, Pergamon Press New York, (1986).

[26] SOIZE C., HUTIN P. M., DESANTI A. and DAVID J. M. – (1) *Rayonnement acoustique des coques dans le domaine MF et extension du programme ADINA en couplage fluide-structure.* RT ONERA 27/3454 RY 063 R, (1983). (2) *Développement d'une méthode de calcul du couplage fluide-structure en moyenne fréquence.* RT ONERA 28/3454 RY 071 R, (1983). (3) *Étude dynamique moyenne fréquence de la poutre tubulaire, à sec et en immersion, dans plusieurs configurations, et comparaisons expérimentales.* RT ONERA 34/3454 RY 081 R, (1984).

[27] ZABREYKO P. P. et al. – *Integral equations—a reference text.* Noordhoff International Publishing, (1975).

[28] ZIENKIEWICZ O. C. – *La méthode des éléments finis.* Ediscience, Paris, (1973).

[29] WILTON D. T. – *Acoustic radiation and scattering from elastic structures.* Inter. Journ. for Numerical Methods in Engin., vol. 13, (1978).